# Nonvolatile Resistance Switching on Two-Dimensional Electron Gas

Jin Gwan Joung,[†] Shin-Ik Kim,[†,‡] Seon Young Moon,[†] Dai-Hong Kim,[§] Hyo Jin Gwon,[†] Seong-Hyeon Hong,[§] Hye Jung Chang,[||] Jin-Ha Hwang,[⊥] Beom Jin Kwon,[†] Seong Keun Kim,[†] Ji-Won Choi,[†] Seok-Jin Yoon,[†] Chong-Yun Kang,[†,#] Kwang Soo Yoo,[∇] Jin-Sang Kim,[†] and Seung-Hyub Baek*,[†,‡]

[†]Electronic Materials Research Center, Korea Institute of Science and Technology, Seoul 136-791, Republic of Korea

[‡]Department of Nanomaterials Science and Technology, Korea University of Science and Technology, Daejeon 305-333, Republic of Korea

[§]Department of Materials Science and Engineering, Research Institute of Advanced Materials Seoul National University, Seoul 151-744, Republic of Korea

[||]Advanced Analysis Center, Korea Institute of Science and Technology, Seoul 136-791, Republic of Korea

[⊥]Department of Materials Science and Engineering, Hongik University, Seoul 121-791, Republic of Korea

[#]KU-KIST Graduate School of Converging Science and Technology, Korea University, Seoul 136-701, Republic of Korea

[∇]Department of Materials Science and Engineering, University of Seoul, Seoul 130-743, Republic of Korea

**S** *Supporting Information*

**ABSTRACT:** Two-dimensional electron gas (2DEG) at the complex oxide interfaces have brought about considerable interest for the application of the next-generation multifunctional oxide electronics due to the exotic properties that do not exist in the bulk. In this study, we report the integration of 2DEG into the nonvolatile resistance switching cell as a bottom electrode, where the metal–insulator transition of 2DEG by an external field serves to significantly reduce the OFF-state leakage current while enhancing the on/off ratio. Using the $Pt/Ta_2O_{5-y}/Ta_2O_{5-x}/SrTiO_3$ heterostructure as a model system, we demonstrate the nonvolatile resistance switching memory cell with a large on/off ratio ($>10^6$) and a low leakage current at the OFF state ($\sim 10^{-13}$ A). Beyond exploring nonvolatile memory, our work also provides an excellent framework for exploring the fundamental understanding of novel physics in which electronic and ionic processes are coupled in the complex heterostructures.

**KEYWORDS:** *two-dimensional electron gas, complex oxide, heterointerface, resistance switching, nonvolatile memory*
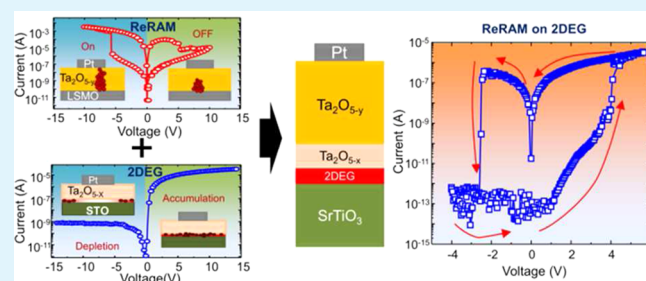
## INTRODUCTION

Heterointerface of multifunctional oxides has provided a fascinating platform to explore the emergent physical properties that do not exist in the bulk.[1] The discovery of two-dimensional electron gas (2DEG) at the interfaces between two insulating $LaAlO_3$ (LAO) and $SrTiO_3$ (STO) layers has brought about intensive experimental and theoretical studies on the physics and applications of this new phenomenon.[2] The most distinct features of 2DEG at an oxide interface over the conventional 2DEG at a semiconductor interface is the functionality: diverse phenomena such as magnetism,[3] superconductivity,[4−6] enhanced capacitance,[7] strong spin−orbit coupling,[8] electron correlation,[9] and nanoscale modulation of 2DEG conductivity[10] have been observed at the oxide interfaces and are promising for the development of multifunctional devices.[10−14]

Among many versatile characteristics of 2DEG at the oxide interface, the metal−insulator transition may be the most intriguing property in the sense that it can be straightforwardly

implemented in logic and memory devices.[10,15−18] The carrier concentration of the 2DEG can be electrostatically tuned by an electric field through accumulation and depletion. This allows us to utilize 2DEG as a channel layer in the structure of three-terminal field-effect transistor.[16,17] The major concern of this type of device is how to control the horizontal transport property of electron carriers in 2DEG layer by the external electric field. However, there are few studies about the effect of the 2DEG metal−insulator transition on the electrical transport property along the vertical direction.[12,19,20] Here, we report a resistance switching memory device integrated on 2DEG at oxide interface, exploring a new opportunity to utilize 2DEG as a bottom electrode having metal−insulator transition property,
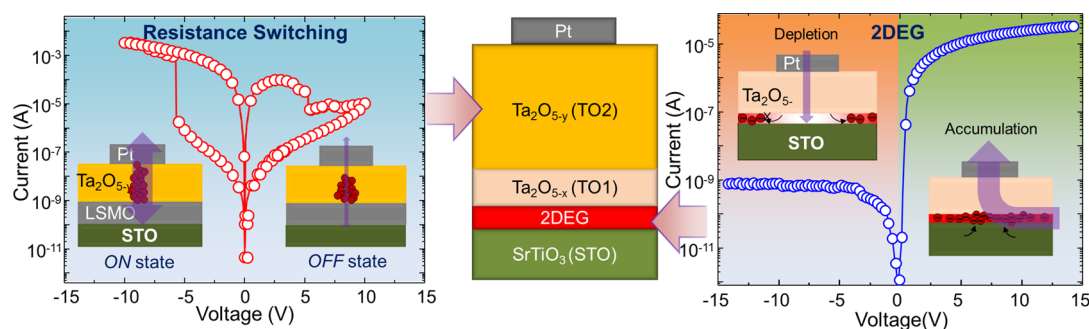
**Figure 1.** Schematic illustration of the integration of the resistance switching device onto 2DEG using the heterostructure of $Pt/Ta_2O_{5-y}/Ta_2O_{5-x}/STO$ as a model system. LSMO stands for $La_{0.33}Sr_{0.67}MnO_3$ conducting oxide layer as a bottom electrode. The arrow shows the direction and the amount of electron flow. (left) $Ta_2O_{5-y}$ layer shows a typical bipolar resistance switching behavior. (right) $Ta_2O_{5-x}$ layer can create 2DEG at the interface with STO. $I-V$ curve shows a diode-like behavior. The dominant origin of such diode-like behavior is the field-effect accumulation and depletion process of 2DEG rather than the Shottky junction (Supporting Information).
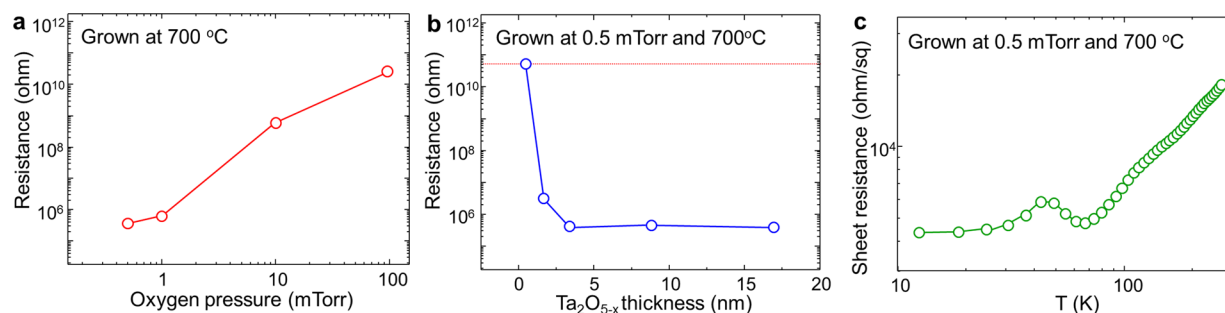


**Figure 2.** Electrical properties of 2DEG at the $Ta_2O_{5-x}$ (TO1)/STO interfaces. (a) Oxygen pressure dependence of the interfacial conductivity. The thickness of the TO1 layer is 10 nm. (b) Critical thickness of TO1 layer to form 2DEG at the interface. (c) Temperature dependence of sheet resistance.

which provides an extra knob to effectively control the electrical transport along the vertical direction.

Resistance switching random access memory (ReRAM) is a promising candidate for next-generation nonvolatile memory devices.[21-32] It can be reversibly switchable from a low resistance state (ON) to a high resistance state (OFF) by an applied electric field. Conducting paths (usually a filamentary form) can be formed and erased through the voltage-driven transport of mobile defects such as oxygen vacancies. One of the key advantages of this memory over the conventional dynamic random access memory (DRAM) is an excellent scalability: this can be achieved by (1) cell size reduction and (2) high-density integration. The two-terminal, vertical capacitor structure of ReRAM cells is much more favorable for the size reduction. Also, as the active switching part is the one-dimensional (1D)-like filament, the switching performance of individual cells does not deteriorate, even when the cell size shrinks down to sub-5 nm scale.[33] Such nanometer-scale ReRAM cells can be integrated with a very high density using a cross-bar array structure.[34]

As the resistance (current flow) is the state variable in the ReRAM, Joule heating is inevitable during operation.[35,36] As the integration density increases, Joule heating becomes a major issue to hamper the further scale-down with the high-density integration. For the unipolar resistance switching devices, the reduction of the RESET current has been a major issue to suppress the heat generation. For example, previous works showed that the RESET current can be reduced by using a nanowire as a resistance switching material,[37] a smaller size of the electrode,[38] and acceptor doping.[39] Also, for both unipolar and bipolar resistance switching devices, a great effort has been

made to remove the sneak path problem in the cross-bar array. The sneak current path is detrimental to the realization of ReRAM not only for the misinterpretation of the stored information, but also for the large heat generation by Joule heating. Previous reports show that this issue can be overcome by engineering $I-V$ characteristic in such a way as to enhance the nonlinearity,[30] inserting metal-insulator transition layers,[23,31] and adding a diode layer.[29,34] Although such a sneak current issue at a circuit level is solved, the Joule heating from the single cell during operation at a cell level still exists.

In order to further solve the heat generation issue of the resistance switching cell, it is desirable to reduce the current flow level during operation. However, the ON-state current has a limitation for the reduction: it should be large enough to distinguish the ON-state from the OFF-state and to obtain the reasonably high operational speed. Thus, a promising strategy would be reducing the OFF-state current while enhancing the on/off ratio. The conventional structure of resistance switching cell has a vertical capacitor structure of metal/insulator/metal. In this structure, the current level at OFF state is determined mainly by the leakage current through the oxide layer. As the resistance switching layer is usually thin with a thickness of around a few tens of nanometers, the leakage current is inevitable. Previous reports showed that doping can be an effective way to reduce the leakage current level of the bipolar resistance switching cell at OFF state.[40,41]

In this study, we demonstrate the resistance switching memory built on 2DEG with low leakage current at OFF state ($\sim10^{-13}$ A) and high on/off ratio ($>10^6$). We fabricate a heterostructure of $Pt/Ta_2O_{5-y}$ (TO2)/$Ta_2O_{5-x}$ (TO1)/STO as a model system (Figure 1). Tantalum oxide is one of the
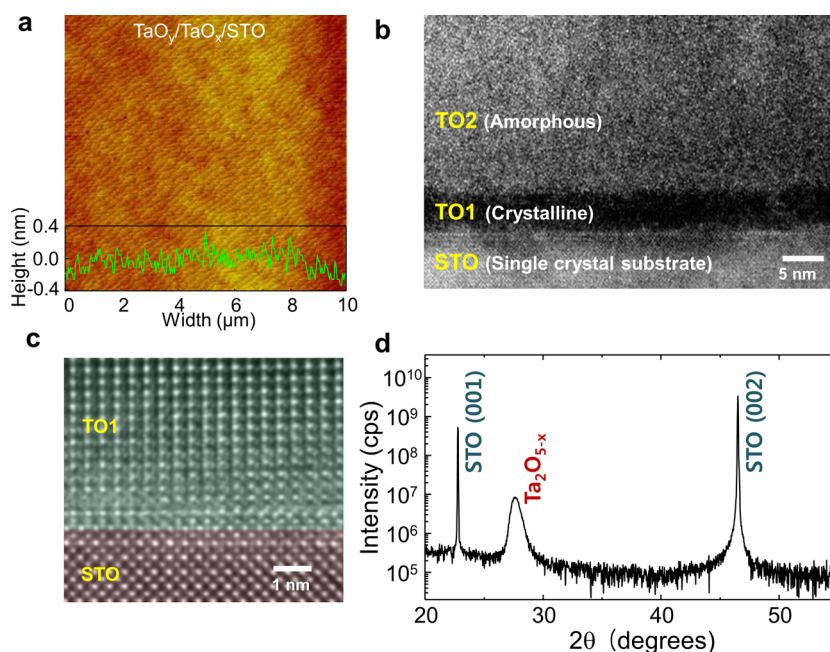
**Figure 3.** Structural characterization of the $Ta_2O_{5-y}/Ta_2O_{5-x}/STO$ structure. (a) The surface morphology of $Ta_2O_{5-y}$ surface measured by AFM. (b) Cross-sectional TEM image. (c) HRTEM image of $Ta_2O_{5-x}/STO$ interface. The image is artificially colored for better visibility. (d) Out-of-plane $\theta-2\theta$ HRXRD scan of $Ta_2O_{5-x}/STO$.

representative materials for the resistance switching. In this structure, TO2 is the main resistance switching layer to determine the total resistance of the cell by forming and erasing the conducting path. STO provides a platform to create 2DEG when TO1 overlayer is deposited on top of it. The 2DEG formed at the TO1/STO interface acts not only as a bottom electrode but also as a metal−insulator transition layer to block the leakage current. A key aspect of the present study is to synthesize two distinct tantalum oxide layers on STO single crystal substrate: the deposition parameters of pulsed laser deposition (PLD) technique have to be precisely controlled to create the 2DEG (TO1/STO interface) and the resistance switching layer (TO2) in the same sample.

## ■ RESULTS AND DISCUSSION

In order to create a conducting interface at the TO1/STO interface, it is critical to grow the tantalum oxide layer at low oxygen pressure (Figure 2a). The TO1 layer grown under the low oxygen pressure (< ~1 mTorr) shows a metallic conductivity, while the one grown under the high oxygen pressure (> ~1 mTorr) exhibits an insulating interface. As tantalum oxide is a nonpolar material, 2DEG cannot be created by the electron reconstruction model which is originally proposed as the major mechanism of 2DEG formation.[2] Rather, it can be more suited to the oxygen vacancy model, where the oxygen vacancies formed on the STO surface during TO1 deposition create the two-dimensional (2D) conducting layer by the doping effect. This is now generally accepted as another mechanism of 2DEG formation.[42−44] To verify the interfacial confinement of the conducting layer, we investigate the thickness effect of TO1 layer to the electrical resistance of the conducting layer. Figure 2b shows two distinct features on the 2D confinement of the conducting layer. First, the resistance of the conducting layer stays the same while the thickness of TO1 layer increases. This indicates that the electrical conductivity we observe is not from the bulk TO1

layer. Second, there exists a critical thickness of ~3 nm to create the electrical conductivity. This is a typical signature of the 2DEG formed at the oxide interface.[2] These results can rule out the possibility of the bulk conduction through TO1 layer. Also, the low-temperature electrical transport behavior of the TO1 (grown at 0.5 mTorr)/STO interface shows a metallic behavior, which is consistent with the previous reports on LAO/STO interface[2,3] (Figure 2c). These results indicate that the electrical conductivity is confined only at the 2D interface. Therefore, we use TO1 layer grown at 700 °C under 0.5 mTorr to create 2DEG at the TO1/STO interface.

The TO2 resistance switching overlayer is grown at 200 °C under oxygen pressure of 70 mTorr: the growth temperature is lowered and the oxygen pressure is increased compared to the growth conditions of TO1 layer. This TO2 layer shows a good resistance switching behavior in the $Pt/TO2/La_{0.67}Sr_{0.33}MnO_3/STO$ heterostructure, as shown in Figure 1, where $La_{0.67}Sr_{0.33}MnO_3$ is a metallic bottom electrode. XRD and TEM analyses show that TO2 layer is amorphous. Usually, the amorphous state is favorable for resistance switching over the crystalline state because the defects such as oxygen vacancy can be easily transported through the loosely bonded, randomly arranged atomic structure in the amorphous materials.

Figure 3a shows an atomic force microscope (AFM) image of the TO2 (50 nm)/TO1 (4 nm)/STO surface. The surface is atomically smooth with flat terraces and steps with a height of ~4 Å, preserving the surface morphology of bare STO substrate. Figure 3b is a bright-field cross-sectional transmission electron microscopy (TEM) image along the [100] zone axis of STO substrate, exhibiting the clear interfaces between each layer. TO1 layer is grown on the top of $TiO_2$-terminated (001) STO single crystal substrate at 700 °C under oxygen pressure of 0.5 mTorr (the details are described in the Methods section). Energy dispersive X-ray spectroscopy (EDAX) analysis on the TO1 layer shows that the atomic ratio of O to Ta is ~2.4. Therefore, it would be reasonable that the TO1

layer is an oxygen-deficient Ta$_2$O$_5$, hence Ta$_2$O$_{5-x}$, as it is grown at low oxygen pressure (0.5 mTorr).

High-resolution TEM and high-resolution X-ray diffraction (XRD) analyses reveal that TO1 is epitaxially grown on STO substrate (Figure 3c,d). Also, multiple domains are observed by high-resolution TEM. However, the exact determination of the TO1 crystal structure is hampered by the lack of the crystallographic data. Tantalum oxide films showing X-ray diffraction peak at 2$\theta$ = ~27.5° (Figure 3d) are often reported as the unidentified phase due to the absence of the crystallographic database.[45,46] This may be attributed to the complexity of tantalum oxides with many possible oxidation states and to the nonstoichiometric films due to the formation of oxygen vacancies during growth.

Electrical transport property in Pt/TO2/TO1/STO heterostructure is characterized as shown in Figure 4a. The current
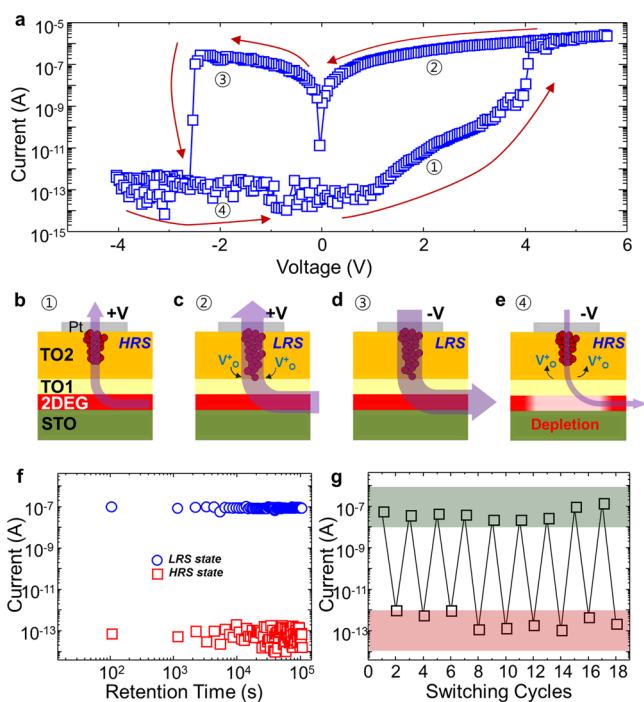


**Figure 4.** Electrical characterization of the Pt/Ta$_2$O$_{5-y}$/Ta$_2$O$_{5-x}$/STO device. (a) Current versus voltage measurement between 25 $\mu$m diameter Pt top and 2DEG bottom electrode. (b−e) The schematic illustration of four distinct states corresponding to those marked by numbers in panel a. The purple arrow and thickness stand for the direction of electron flow and current level, respectively. HRS stands for high resistance state with the conducting filament disconnected, while LRS stands for low resistance state with the filament connected. V$_O^+$ stands for the oxygen vacancy. (f) Retention property of HRS and LRS. After switching, the current is measured at −1 V of reading voltage for more than 24 h. (g) Reversible resistance switching measured at −1 V of reading voltage. All the electrical measurement was done at room temperature.

flow is measured as a function of the applied electric field between the top Pt electrode with a 25 $\mu$m diameter and the bottom 2DEG electrodes. The I−V curve shows a hysteretic behavior typically shown in bipolar resistance switching memory. It is remarkable that the OFF-state current is significantly suppressed when the negative field is applied on top electrode. This result is a combination of two different effects: (1) bipolar resistance switching in the TO2 layer and (2) electric-field-driven metal−insulator transition in 2DEG

layer. Figure 4b−e shows the schematic illustrations to explain the transport properties at four distinct states in a single switching cycle (panels b−e correspond to each state marked by numbers in panel a). The SET occurs at the positive voltage in the Pt/TO2/TO1/STO sample while it does at the negative voltage in the Pt/TO2/LSMO/STO. This indicates that the location of the forming and rupturing of the conducting filaments in the Pt/TO2/TO1/STO sample is close to the bottom 2DEG, as marked in Figure 4b−e. As the oxygen vacancies are positively charged, upon the positive voltage on the top electrode, they move toward the TO2/TO1 interface to form a conducting filament (Figure 4c). On the other hand, when the negative voltage is applied, the oxygen vacancies are attracted toward the Pt/TO2 interface, destroying the connection of the conducting filament at the TO2/TO1 interface (Figure 4e).

When the positive voltage is applied on the top electrode, the device structure becomes identical to metal/insulator/metal, which is the same as the conventional resistance switching cell. This is because the 2DEG layer works as a metallic electrode at the positive voltage regime. Figure 4b shows the schematic illustration of the OFF state under the positive electric field on the top electrode. In this state, the overall resistance state is high due to the disconnected filament. However, it is noted that the current flow is increased with the applied positive voltage. This is attributed to the leakage current through the tantalum oxide layers and the increased carrier concentration of the 2DEG layer by accumulation. At around +4 V, "switching ON" happens with the filament connected at TO2 layer, resulting in a sharp increase of the current level by around 2 orders of magnitude. At this ON state, the applied positive voltage can drive electrons to move from the 2DEG layer to the Pt top electrode through the filamentary path in the TO2 layer, hence the low resistance state (Figure 4c). Therefore, in the positive voltage regime, the overall resistance switching behavior of our device is almost same as that of the conventional one. However, when the negative field is applied on the top electrode, the switching behavior becomes different, as discussed below.

The negative voltage applied on the top electrode at the ON state drives electrons to move in the opposite direction, that is, from Pt to 2DEG electrodes through the conducting filament. As the TO2 layer behaves like a conductor at the ON state, the applied negative voltage is mainly consumed by the current flow, and hence the field effect on 2DEG becomes negligible. This means that 2DEG still can serve as a bottom electrode without depletion (Figure 4d). This is supported by the almost symmetrical shape of the ON-state current in the range from −2 V to +2 V, as shown in Figure 4a. Therefore, the low resistance (ON) state turned on at the positive voltage regime can be equally readable by applying the low negative reading voltage.

At around −2.5 V, "switching OFF" occurs with the filament disconnected at TO2 layer, resulting in a sharp decrease of the current level. There are two distinct features in the switching OFF process: (1) the current level is significantly decreased by more than 6 orders of magnitude, and (2) the current level stays almost same at ~10$^{-13}$ A (measurement limit), despite the increase of the negative voltage. This is due to the metal−insulator transition of 2DEG via depletion. At the OFF state, the TO2 layer becomes an insulator, and it can deliver the electrostatic field applied on the top electrode into the 2DEG layer in the same way as the gate oxide does in the field-effect transistor. Then, the negative field on the top electrode can

electrostatically deplete the electron carriers in the 2DEG layer. The depletion of 2DEG effectively corresponds to the disappearance of the bottom electrode in our device geometry (Figure 4e). This can lead to the significant suppression of the OFF-state current as well as a substantial enhancement of on/off ratio (> ~$10^6$), as shown in Figure 4a.

It would be interesting to compare the resistance switching behavior of our Pt/TO2/TO1/STO device with that of the Pt/TO2/LSMO/STO device (Figure 1) with a conventional M/I/M structure, where the resistance switching layer is grown at the same condition for both samples. The Pt/TO2/LSMO/STO sample shows a bipolar resistance switching behavior with ~$10^4$ of the on/off ratio and ~$10^{-8}$A of the OFF-state current at ±1 V, as shown in Figure 1.Therefore, it is clear that the OFF-state current is significantly suppressed with the enhancement of on/off ratio utilizing the field-effect metal−insulator transition of 2DEG.

To evaluate the retention property, we monitor both high and low resistance states as a function of time, as shown in Figure 4f. The ON and OFF states are set by applying +5 V and −5 V, respectively, and then the electric current is measured at −1 V of reading voltage. Both states prove stable over $10^5$ seconds of investigation without any relaxation. A previous report showed that the low current operation (<10 $\mu$A) of tantalum oxide-based resistance switching cells causes the severe degradation of the retention property compared to the high current operation.[47] Our device exhibits a very strong retention property even below nA level. Also, the resistance state can be reversibly switchable, as shown in Figure 4g.

Novel oxide electronic devices can be further envisaged using our approach to integrate the 2DEG at oxide interface to the resistance switching device. For example, many functionalities arising from the STO-based 2DEG, such as optical, magnetic, and chemical characteristics, can be potentially utilized to realize a multifunctional oxide electronic device. Also, a logic device with built-in nonvolatile memory could be possible in which 2DEG can be used as a channel layer in the transistor. However, there are some issues to be solved. For example, the carrier mobility of the electron carriers in the 2DEG is not high at room temperature, and hence, the resistance of 2DEG is relatively high. This may limit the operational speed and increase the switching voltage.[48] Also, it should be noted that our device as-is will have a sneak path problem when it is integrated with the cross-bar array. However, previous works show that the sneak path problem can be solved by integrating a diode to the resistance switching device.[34] We believe that the same approach can be possible with our device.

## CONCLUSIONS

In summary, we have demonstrated the 2DEG-integrated resistance switching memory to suppress the OFF-state current while maintaining high on/off ratio. Our approach can significantly enhance the integration density of the resistance switching cells by reducing the heat generation arising from the leakage current. Our work shows that the metal−insulator transition of 2DEG by an electric field can be used to actively control the electrical transport in the vertical capacitor structure. Beyond resistance switching memory, our approach will open new opportunities to develop the multifunctional nanoelectronics utilizing a wide spectrum of 2DEG properties operating with other parameters such as magnetism, light, and spin. Moreover, our work provides an excellent platform to explore fundamental understanding on novel physics where electronic and ionic processes are coupled in ultrathin heterostructures.

## METHODS

**Film Growth.** First, (001) STO single crystal substrates were etched by BHF. Then, they were annealed at 1000 °C under oxygen environment to make the TiO$_2$-terminated surface with the clean step-and-terrace structure. Tantalum oxide films were deposited on this substrate by pulsed laser deposition (PLD) technique. The substrates were attached to a resistive heater and positioned 50 mm from the stoichiometric Ta$_2$O$_5$ target. A KrF excimer laser beam ($\lambda$ = 248 nm) was used with an energy density of 1.5 J/cm$^2$ and a frequency of 2 Hz. Ta$_2$O$_{5-x}$ (TO1) was grown at a substrate temperature of 700 °C under oxygen pressure of 0.5 mTorr. Subsequently, Ta$_2$O$_{5-y}$ (TO2) thin films were grown at a substrate temperature of 200 °C under oxygen pressure ranging from 70 to 100 mTorr.

**Characterization.** The surface morphology was characterized using a commercial atomic force microscope (AFM, Digital Instruments Dimension 3100 equipped with a Nanoscope IV controller) under tapping mode. The stoichiometry of thin film is analyzed using an FEI Tecnai F20G2 microscope equipped with the energy dispersive X-ray spectroscopy (PV9761/55 ME). High-resolution transmission electron microscopy analysis was carried out using a FEI Titan 80−300 microscope operated at an accelerating voltage of 300 keV. The available point resolution is better than 1.3 Å at an operating accelerating voltage. Images were recorded by a 2k × 2k CCD (Gatan, US1000) camera. A Keithley 4200 SCS semiconductor characterization system was used to perform the resistive switching measurement with contacts to devices made using a probe station. Pt electrodes were deposited on samples by sputtering at room temperature after patterning the bottom lines by photolithography (MDA-400M) and then using a lift-off method.

## ASSOCIATED CONTENT

**Ⓢ Supporting Information**

Cycling test of Pt/TO2/TO1/STO structure, $C−V$ curve of Pt/TO1/STO, electrical contact methods, and $I−V$ curve of 2DEG. This material is available free of charge via the Internet at http://pubs.acs.org.

## AUTHOR INFORMATION

**Corresponding Author**
*E-mail: shbaek77@kist.re.kr. Fax: +82-2-958-6720. Tel: +82-2-958-5382.

**Author Contributions**

J.G.J. fabricated samples and prepared the manuscript. D.H.K., S.H.H., and H.J.C. performed the structural analyses by XRD and TEM. S.Y.M. characterized the low-temperature electrical property. S.I.K. and H.J.G. supported the sample fabrication. J.H.H., B.J.K., S.K.K., J.W.C., S.J.Y., and C.Y.K. provided the theoretical analysis. K.S.Y., J.S.K., and S.H.B. supervised the study. S.H.B. designed and directed the research. All authors discussed the results and implications and commented on the manuscript at all stages.

## ■ REFERENCES

(1) Hwang, H. Y.; Iwasa, Y.; Kawasaki, M.; Keimer, B.; Nagaosa, N.; Tokura, Y. Emergent Phenomena at Oxide Interfaces. *Nat. Mater.* **2012**, *11*, 103−113.

(2) Ohtomo, A.; Hwang, H. Y. A High-Mobility Electron Gas at the LaAlO₃/SrTiO₃ Heterointerface. *Nature* **2004**, *427*, 423−426.

(3) Brinkman, A.; Huijben, M.; van Zalk, M.; Huijben, J.; Zeitler, U.; Maan, J. C.; van der Wiel, W. G.; Rijnders, G.; Blank, D. H.; Hilgenkamp, H. Magnetic Effects at the Interface between Non-Magnetic Oxides. *Nat. Mater.* **2007**, *6*, 493−496.

(4) Reyren, N.; Thiel, S.; Caviglia, A. D.; Kourkoutis, L. F.; Hammerl, G.; Richter, C.; Schneider, C. W.; Kopp, T.; Ruetschi, A. S.; Jaccard, D.; Gabay, M.; Muller, D. A.; Triscone, J. M.; Mannhart, J. Superconducting Interfaces between Insulating Oxides. *Science* **2007**, *317*, 1196−1199.

(5) Bert, J. A.; Kalisky, B.; Bell, C.; Kim, M.; Hikita, Y.; Hwang, H. Y.; Moler, K. A. Direct Imaging of the Coexistence of Ferromagnetism and Superconductivity at the LaAlO₃/SrTiO₃ Interface. *Nat. Phys.* **2011**, *7*, 767−771.

(6) Li, L.; Richter, C.; Mannhart, J.; Ashoori, R. C. Coexistence of Magnetic Order and Two-Dimensional Superconductivity at LaAlO₃/SrTiO₃ Interfaces. *Nat. Phys.* **2011**, *7*, 762−766.

(7) Li, L.; Richter, C.; Paetel, S.; Kopp, T.; Mannhart, J.; Ashoori, R. C. Very Large Capacitance Enhancement in a Two-Dimensional Electron System. *Science* **2011**, *332*, 825−828.

(8) Caviglia, A. D.; Gabay, M.; Gariglio, S.; Reyren, N.; Cancellieri, C.; Triscone, J. M. Tunable Rashba Spin-Orbit Interaction at Oxide Interfaces. *Phys. Rev. Lett.* **2010**, *104*, 126803.

(9) Jang, H. W.; Felker, D. A.; Bark, C. W.; Wang, Y.; Niranjan, M. K.; Nelson, C. T.; Zhang, Y.; Su, D.; Folkman, C. M.; Baek, S. H.; Lee, S.; Janicka, K.; Zhu, Y.; Pan, X. Q.; Fong, D. D.; Tsymbal, E. Y.; Rzchowski, M. S.; Eom, C. B. Metallic and Insulating Oxide Interfaces Controlled by Electronic Correlations. *Science* **2011**, *331*, 886−889.

(10) Cen, C.; Thiel, S.; Mannhart, J.; Levy, J. Oxide Nanoelectronics on Demand. *Science* **2009**, *323*, 1026−1030.

(11) Kim, S. I.; Kim, D. H.; Kim, Y.; Moon, S. Y.; Kang, M. G.; Choi, J. K.; Jang, H. W.; Kim, S. K.; Choi, J. W.; Yoon, S. J.; Chang, H. J.; Kang, C. Y.; Lee, S.; Hong, S. H.; Kim, J. S.; Baek, S. H. Non-Volatile Control of 2DEG Conductivity at Oxide Interfaces. *Adv. Mater.* **2013**, *25*, 4612−4617.

(12) Wu, S. X.; Luo, X.; Turner, S.; Peng, H. Y.; Lin, W. N.; Ding, J. F.; David, A.; Wang, B. A.; Van Tendeloo, G.; Wang, J. L.; Wu, T. Nonvolatile Resistive Switching in Pt/LaAlO₃/SrTiO₃ Heterostructures. *Phys. Rev. X* **2013**, *3*, 041027.

(13) Irvin, P.; Ma, Y. J.; Bogorin, D. F.; Cen, C.; Bark, C. W.; Folkman, C. M.; Eom, C. B.; Levy, J. Rewritable Nanoscale Oxide Photodetector. *Nat. Photonics.* **2010**, *4*, 849−852.

(14) Xie, Y.; Bell, C.; Hikita, Y.; Hwang, H. Y. Tuning the Electron Gas at an Oxide Heterointerface via Free Surface Charges. *Adv. Mater.* **2011**, *23*, 1744−1747.

(15) Thiel, S.; Hammerl, G.; Schmehl, A.; Schneider, C. W.; Mannhart, J. Tunable Quasi-Two-Dimensional Electron Gases in Oxide Heterostructures. *Science* **2006**, *313*, 1942−1945.

(16) Förg, B.; Richter, C.; Mannhart, J. Field-Effect Devices Utilizing LaAlO₃−SrTiO₃ Interfaces. *Appl. Phys. Lett.* **2012**, *100*, 053506.

(17) Hosoda, M.; Hikita, Y.; Hwang, H. Y.; Bell, C. Transistor Operation and Mobility Enhancement in Top-Gated LaAlO₃/SrTiO₃ Heterostructures. *Appl. Phys. Lett.* **2013**, *103*, 103507.

(18) Bark, C. W.; Sharma, P.; Wang, Y.; Baek, S. H.; Lee, S.; Ryu, S.; Folkman, C. M.; Paudel, T. R.; Kumar, A.; Kalinin, S. V.; Sokolov, A.; Tsymbal, E. Y.; Rzchowski, M. S.; Gruverman, A.; Eom, C. B. Switchable Induced Polarization in LaAlO₃/SrTiO₃ Heterostructures. *Nano Lett.* **2012**, *12*, 1765−1771.

(19) Kim, S. K.; Kim, S. I.; Hwang, J. H.; Kim, J. S.; Baek, S. H. Capacitance−Voltage Analysis of LaAlO₃/SrTiO₃ Heterostructures. *Appl. Phys. Lett.* **2013**, *102*, 112906.

(20) Singh-Bhalla, G.; Bell, C.; Ravichandran, J.; Siemons, W.; Hikita, Y.; Salahuddin, S.; Hebard, A. F.; Hwang, H. Y.; Ramesh, R. Built-In and Induced Polarization across LaAlO₃/SrTiO₃ Heterojunctions. *Nat. Phys.* **2011**, *7*, 80−86.

(21) Waser, R.; Dittmann, R.; Staikov, G.; Szot, K. Redox-Based Resistive Switching Memories—Nanoionic Mechanisms, Prospects, and Challenges. *Adv. Mater.* **2009**, *21*, 2632−2663.

(22) Kim, K. M.; Jeong, D. S.; Hwang, C. S. Nanofilamentary Resistive Switching in Binary Oxide System; A Review on the Present Status and Outlook. *Nanotechnology* **2011**, *22*, 254002.

(23) Son, M.; Liu, X.; Sadaf, S. M.; Lee, D.; Park, S.; Lee, W.; Kim, S.; Park, J.; Shin, J.; Jung, S.; Ham, M. H.; Hwang, H. Self-Selective Characteristics of Nanoscale VOₓ Devices for High-Density ReRAM Applications. *IEEE Electron Device Lett.* **2012**, *33*, 718−720.

(24) Lee, M. J.; Lee, C. B.; Lee, D.; Lee, S. R.; Chang, M.; Hur, J. H.; Kim, Y. B.; Kim, C. J.; Seo, D. H.; Seo, S.; Chung, U. I.; Yoo, I. K.; Kim, K. a Fast, High-Endurance, and Scalable Non-Volatile Memory Device Made from Asymmetric Ta₂O₅₋ₓ/TaO₂₋ₓ Bilayer Structures. *Nat. Mater.* **2011**, *10*, 625−630.

(25) Linn, E.; Rosezin, R.; Kugeler, C.; Waser, R. Complementary Resistive Switched for Passive Nanocrossbar Memories. *Nat. Mater.* **2010**, *9*, 403−406.

(26) Wei, Z.; Kanzawa, Y.; Arita, K.; Katoh, Y.; Kawai, K.; Muraoka, S.; Mitani, S.; Fujii, S.; Katayama, K.; Iijima, M.; Mikawa, T.; Ninomiya, T.; Miyanaga, R.; Kawashima, Y.; Tsuji, K.; Himeno, A.; Okada, T.; Azuma, R.; Shimakawa, K.; Sugaya, H.; Takagi, T.; Yasuhara, R.; Horiba, K.; Kumigashira, H.; Oshima, M. Highly Reliable TaOₓ ReRAM and Direct Evidence of Redox Reaction Mechanism. *IEEE Int. Electron Devices Meet.* **2008**, 293−296.

(27) Park, G. S.; Kim, Y. B.; Park, S. Y.; Li, X. S.; Heo, S.; Lee, M. J.; Chang, M.; Kwon, J. H.; Chung, U. I.; Dittmann, R.; Waser, R.; Kim, K. In Situ Observation of Filamentary Conducting Channels in an Asymmetric Ta₂O₅₋ₓ/TaO₂₋ₓ Bilayer Structure. *Nat. Commun.* **2013**, *4*, 2382.

(28) Bai, Y.; Wu, H.; Wu, R.; Zhang, Y.; Deng, N.; Yu, Z.; Qian, H. Study of Multi-Level Characteristics for 3D Vertical Resistive Switching Memory. *Sci. Rep.* **2014**, *4*, 5780.

(29) Yang, J. J.; Borghetti, J.; Murphy, D.; Stewart, D. R.; Williams, R. S. A Family of Electronically Reconfigurable Nanodevices. *Adv. Mater.* **2009**, *21*, 3754−3758.

(30) Yang, J. J.; Zhang, M. X.; Pickett, M. D.; Miao, F.; Strachan, J. P.; Li, W. D.; Yi, W.; Ohlberg, D. A. A.; Choi, B. J.; Wu, W.; Nickel, J. H.; Medeiros-Ribeiro, G.; Williams, R. S. Engineering Nonlinearity into Memristors for Passive Crossbar Applications. *Appl. Phys. Lett.* **2012**, *100*, 113501.

(31) Chang, S. H.; Lee, S. B.; Jeon, D. Y.; Park, S. J.; Kim, G. T.; Yang, S. M.; Chae, S. C.; Yoo, H. K.; Kang, B. S.; Lee, M. J.; Noh, T. W. Oxide Double-Layer Nanocrossbar for Ultrahigh-Density Bipolar Resistive Memory. *Adv. Mater.* **2011**, *23*, 4063−4067.

(32) Yang, J. J.; Zhang, M. X.; Strachan, J. P.; Miao, F.; Pickett, M. D.; Kelley, R. D.; Medeiros-Ribeiro, G.; Stanley Williams, R. High Switching Endurance in TaOₓ Memristive Devices. *Appl. Phys. Lett.* **2010**, *97*, 232102.

(33) Park, J.; Lee, W.; Choe, M.; Jung, S.; Son, M.; Kim, S.; Park, S.; Shin, J.; Lee, D.; Siddik, M.; Woo, J.; Choi, G.; Cha, E.; Lee, T.; Hwang, H. Quantized Conductive Filament Formed by Limited Cu Source in Sub-5 nm Era. *2011 IEEE Int. Electron Devices Meet.* **2011**, *63*, 371−374.

(34) Kim, G. H.; Lee, J. H.; Ahn, Y.; Jeon, W.; Song, S. J.; Seok, J. Y.; Yoon, J. H.; Yoon, K. J.; Park, T. J.; Hwang, C. S. 32 × 32 Crossbar Array Resistive Memory Composed of a Stacked Schottky Diode and Unipolar Resistive Memory. *Adv. Funct. Mater.* **2013**, *23*, 1440−1449.

(35) Akinaga, H.; Shima, H. Resistive Random Access Memory (ReRAM) Based on Metal Oxides. *Proc. IEEE* **2010**, *98*, 2237−2251.

(36) Pan, F.; Chen, C.; Wang, Z. S.; Yang, Y. C.; Yang, J.; Zeng, F. Nonvolatile Resistive Switching Memories-Characteristics, Mechanisms and Challenges. *Prog. Nat. Sci.* **2010**, *20*, 1−15.

(37) Kim, S. I.; Lee, J. H.; Chang, Y. W.; Hwang, S. S.; Yoo, K. H. Reversible Resistive Switching Behaviors in NiO Nanowires. *Appl. Phys. Lett.* **2008**, *93*, 033503.

(38) Ahn, S. E.; Lee, M. J.; Park, Y.; Kang, B. S.; Lee, C. B.; Kim, K. H.; Seo, S.; Suh, D. S.; Kim, D. C.; Hur, J.; Xianyu, W.; Stefanovich, G.; Yin, H.; Yoo, I. K.; Lee, J. H.; Park, J. B.; Baek, I. G.; Park, B. H. Write Current Reduction in Transition Metal Oxide Based Resistance-Change Memory. *Adv. Mater.* **2008**, *20*, 924−928.

(39) Lee, S. B.; Kim, A.; Lee, J. S.; Chang, S. H.; Yoo, H. K.; Noh, T. W.; Kahng, B.; Lee, M. J.; Kim, C. J.; Kang, B. S. Reduction of High Reset Currents in Unipolar Resistance Switching Pt/SrTiO$_x$/Pt Capacitors Using Acceptor Doping. *Appl. Phys. Lett.* **2010**, *97*, 093505.

(40) Xu, D. L.; Xiong, Y.; Tang, M. H.; Zeng, B. W.; Li, J. Q.; Liu, L.; Li, L. Q.; Yan, S. A.; Tang, Z. H. Bipolar Resistive Switching Behaviors in Cr-Doped ZnO Films. *Microelectron. Eng.* **2014**, *116*, 22−25.

(41) Guan, W.; Liu, M.; Long, S.; Liu, Q.; Wang, W. On the Resistive Switching Mechanisms of Cu/ZrO$_2$:Cu/Pt. *Appl. Phys. Lett.* **2008**, *93*, 223506.

(42) Chen, Y. Z.; Bovet, N.; Trier, F.; Christensen, D. V.; Qu, F. M.; Andersen, N. H.; Kasama, T.; Zhang, W.; Giraud, R.; Dufouleur, J.; Jespersen, T. S.; Sun, J. R.; Smith, A.; Nygard, J.; Lu, L.; Buchner, B.; Shen, B. G.; Linderoth, S.; Pryds, N. A High-Mobility Two-Dimensional Electron Gas at the Spinel/Perovskite Interface of $\gamma$-Al$_2$O$_3$/SrTiO$_3$. *Nat. Commun.* **2013**, *4*, 1371.

(43) Lee, S. W.; Liu, Y.; Heo, J.; Gordon, R. G. Creation and Control of Two-Dimensional Electron Gas Using Al-Based Amorphous Oxides/SrTiO$_3$ Heterostructures Grown by Atomic Layer Deposition. *Nano Lett.* **2012**, *12*, 4775−4783.

(44) Chen, Y.; Pryds, N.; Kleibeuker, J. E.; Koster, G.; Sun, J.; Stamate, E.; Shen, B.; Rijnders, G.; Linderoth, S. Metallic and Insulating Interfaces of Amorphous SrTiO$_3$-Based Oxide heterostructures. *Nano Lett.* **2011**, *11*, 3774−3778.

(45) Nishimura, Y.; Shinkawa, A.; Ujita, H.; Tsuji, M.; Nakamura, M. Deposition of Tantalum Oxide Films by ArF Excimer Laser Ablation. *Appl. Surf. Sci.* **1998**, *136*, 22−28.

(46) Boughaba, S.; Sproule, G. I.; McCaffrey, J. P.; Islam, M.; Graham, M. J. Synthesis of Tantalum Pentoxide Films by Pulsed Laser Deposition: Material Characterization and Scale-Up. *Thin Solid Films* **2000**, *358*, 104−113.

(47) Prakash, A.; Jana, D.; Maikap, S. TaO$_x$-Based Resistive Switching Memories: Prospective and Challenges. *Nanoscale Res. Lett.* **2013**, *8*, 418.

(48) Shima, H.; Takano, F.; Muramatsu, H.; Akinaga, H.; Tamai, Y.; Inque, I. H.; Takagi, H. Voltage Polarity Dependent Low-Power and High-Speed Resistance Switching in CoO Resistance Random Access Memory with Ta Electrode. *Appl. Phys. Lett.* **2008**, *93*, 113504.